

On-Board Compressor Water Injection for Civil Aircraft Emission Reductions: Range Performance with Fuel Burn Analysis

David Alejandro Block Novelo, Uyioghosa Igie and Devaiah Nalianda

School of Aerospace, Transport and Manufacturing, Cranfield University,

Abstract

The performance benefit of compressor water injection for a stand-alone jet engine has been investigated in previous work conducted by the authors, as well as other studies. For the same required thrust, the benefits include reduced specific fuel consumption, turbine inlet temperature and NO_x emissions. The additional weight implication for aircraft (narrow and wide-body type) with their typical engine type (two and three-spool) for the varied range is investigated here. The emphasis of this study is to establish whether the performance benefit restricted to take-off and parts of the climb, offsets the additional weight penalty of the water injection system, onboard the aircraft. An in-house aircraft performance tool has been used and the changes in performance due to water injection are determined by an evaporation model previously developed. This study shows that the shortest range of 4 missions offers small overall fuel savings of 0.42% per flight cycle. The longest mission, in which the injection equipment is carried for longer (though mostly empty water tank), brings about an overall increase in fuel consumed, by about 0.05%. For the same range, the aircraft powered by a three-spool engine shows better performance. However, both aircraft equally benefit from landing and take-off NO_x emission reductions of around 43%. Water Injection is shown to result in similar performance benefits as 25% take-off derate but without the penalties in fuel burn or increased take-off and climb times. Reductions in turbine inlet temperature obtained are worth considerable attention as a means of decreasing the direct operating costs of an airline.

Keywords: NO_x emissions, Aircraft performance, emissions reductions, water injection. Derated take-off

1- Introduction

Rising levels of air pollutants around airports have become more of a concern and it is a direct consequence of higher air traffic influenced by the increased demand of air travel estimated at 5.3% per year [1]. Block and Igie [2] shows that few measures aimed at reducing airport emissions seem to tackle Nitrogen Oxides (NO_x), and most of them are focused on reducing fuel burn and consequently carbon emissions. The latter can be achieved by reducing the on-time of the engines by means of technological or operational improvements. NO_x reductions, however, are more challenging to tackle as they depend on the temperature and residence time of the gas in the primary combustion zone. During take-off, which is when the highest engine power/thrust is required, NO_x emissions will peak. To limit this, the combustion temperature needs to be lowered. One approach to this is redesigning the combustion chamber to reduce the residence time or the temperature of the combustion process. Modern aero-engines with higher pressure ratios (PR) and Turbine Inlet Temperatures (TIT) give rise to more NO_x emissions. However, advances in combustion chamber design have managed to keep the Emission Indices

(EI) within acceptable levels. For instance, staged combustion offers around a 40-50% reduction in NO_x , compared to conventional burners, and Rich-Burn Quick Quench Lean combustors offer improvements in the range of 50-60% [3,4]. Liu et al. [3] is a comprehensive overview of modern combustion chamber designs, their improvements in NO_x and their development challenges.

Nevertheless, regulations on aero-engine pollutants are becoming more stringent. The sole focus on combustion chamber design improvement is not likely to be sufficient to comply with ICAO long-term emission targets of 60% NO_x emissions reductions by 2026 (compared to 2004)[1]. ICAO forecasts that to keep aircraft emissions within acceptable levels, technological, operational and regulatory improvements, all need to occur simultaneously to counteract the growth of the civil aircraft fleet [1]. Reduced thrust take-off is an operational measure which can also lead to improved take-off NO_x emissions. It has been shown that reducing the take-off thrust can lead to reductions of NO_x emissions estimated at 31%, compared to full thrust take-off [5,6]. Other studies [7,8] suggest reductions of 0.7% NO_x for every 1% of derate, meaning the highest reductions achievable, corresponding to 25% derate (maximum reduction allowed by authorities) would be 17.5%. However, this can come with a fuel burn penalty due to longer take-off and climb times and it is restricted by the runway length and environmental conditions [6]. An alternative solution analysed here is aimed at reducing emissions by cooling the core flow of the engine by means of injecting atomized water droplets into the intermediate pressure compressor (IPC) of the engine. The thermodynamics of compressor performance with water injection has been studied by Refs.[9–11]. Refs. [12–15] offer analytical and experimental performance studies of single-spool gas turbines. However, to the knowledge of the authors, only one group of study incorporates this to aircraft performance. These papers [16,17] analyse a system for a Boeing 747, flying one mission under one ambient condition. The study concludes that misting the compressor with water could lead to NO_x reductions of up to 47%, and this is compared to combustion chamber water injection that offers a greater reduction in NO_x but with a penalty in fuel burn. The aircraft studied in the report represents only 1% of the wide-bodied aircraft (WBA) order backlog as can be observed from Ref [18] for a B747. Based on the fleet and aircraft demand presented on the airliner census [18], operators seem to prefer 2-engine aircraft due to their lower operating cost. The research presented here expands the investigation into two different types of aircraft, both with twin-engines. Also, the influence of range is taken into account by considering missions ranging from 500 to 11,000 km. The narrow-bodied aircraft (NBA) studied here is representative of around 90% of the narrow-body order backlog and used for the short-haul mission (SHM) and medium-haul mission (MHM). The WBA investigated is applicable to long-haul missions (LHM) and MHM, and is representative of nearly 30% of the order backlog for the WBA type aircraft. It is important to highlight that the mode of engine control considered in this study is to keep the required thrust during water injection the same as in the dry case. As such, the potential thrust augmentation does not occur. In another approach which can involve a constant TIT, the fuel flow is expected to rise to maintain the same TIT. As such, higher pressure ratios occur, the Specific Fuel Consumption (SFC) is also reduced as relatively less fuel is used to generate the higher thrust. As TIT is unchanged, the NO_x is expected to remain approximately constant. This approach is not considered here as it does not offer a reduction in NO_x and brings about an increase in the absolute value of fuel used, leading to more CO_2 .

2- Methodology

2.1 Aircraft Performance

The aircraft performance tool implemented here is *Hermes*, a Cranfield University in-house code. The calculation of aircraft performance is based on the Total Energy Model methodology for aircraft performance[19,20]. The inputs for the program are the geometry of the aircraft (airframe length and diameter; span, thickness-to-chord ratio and aspect ratio of the wings and high lift devices configuration), the weight, and the mission specifications. The mission profile is calculated based on defined speeds and altitudes. It solves Newton's second law of motion for the aircraft, equating the propulsive force to the drag (estimated based on the given geometry) and the acceleration. The lift force (calculated from wing geometry) is equated to the weight (airframe, engines, payload and fuel). *Hermes* runs the engine performance tool, *Turbomatch* to calculate the thrust required at each segment, and thus the SFC of the engines and total fuel consumption for the mission. The simplified forces of the aircraft at any flight segment are represented in Fig. 1.

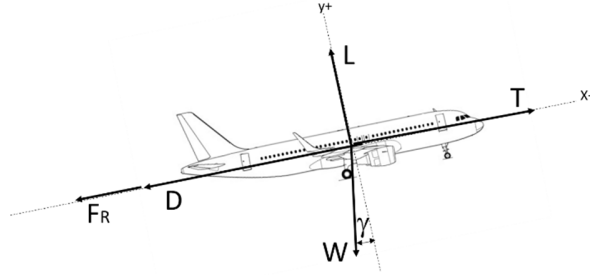


Figure 1 Forces on an Aircraft

Solving the forces on the free body diagram of Fig. 1, two equations can be derived,

$$\Sigma F_x = T - D - F_R - W \sin \gamma = m \left(\frac{dv_x}{dt} \right) \quad (1)$$

$$\Sigma F_y = L - W \cos \gamma = m \left(\frac{dv_y}{dt} \right) \quad (2)$$

T: Is the total aircraft thrust and represents the thrust per engine, multiplied by the number of engines, $T = F_n * n$. This thrust is calculated by an integrated engine performance simulation code: *Turbomatch* by varying the TIT or fuel flow for the different off-design points at which the engine is operating, to satisfy Eq. (1). The thrust value will be maximum at take-off and climb, and minimum at idling and descend. For the cruise condition, the simulations show that cruise thrust is between 15 to 20% of the maximum static take-off thrust value.

D: is the aerodynamic drag and is calculated by adding the zero-lift and lift-induced drag coefficients of each flying element, as explained in Ref. [21]. *Hermes* considers skin friction, interference drag, and profile drag. All the previous is calculated by means of the input geometric parameters and flight conditions. The drag term will always be present as long as the aircraft is moving.

F_R : is the rolling coefficient and can be computed by multiplying the rolling resistance μ_R , by the aircraft reaction R . When the aircraft is on the ground the reaction to the weight is the weight itself (W), so $R=W$ and thus $F_R = \mu_R W$. The rolling resistance μ_R is 0.02 on a paved runway; other values for μ_R can be found in Ref.[20]. Once the wheels leave the ground, this term becomes zero, since the ground reaction gets substituted entirely by the lift force.

W sin γ : In Fig. 2, the axis has been tilted to be aligned with the aircraft trajectory. The aircraft's weight thus has an angle γ with respect to the ground known as climb gradient. When the aircraft is in cruise or taxiing, γ is zero and this term disappears. The climb gradient can also be defined by the ratio of vertical to horizontal speeds where dh is the change in altitude,

$$\sin \gamma = \frac{\left(\frac{dh}{dt}\right)}{V_x} \quad (3)$$

$m \left(\frac{dv_x}{dt}\right)$: is the acceleration term only relevant while the aircraft changes its speed during the take-off roll or descend. During cruise, this term is zero along with $\sin \gamma$ and F_R so that the only two forces in the horizontal plane (x) are the thrust and the drag.

L: Is the lift force, calculated from the geometric parameters of the wings and the defined flight velocities. The lift is dependent on the lift coefficient of the wings, the density of the air, the area of the wings and the flight speed. The aerodynamic efficiency of the lifting surfaces will be evaluated by the lift to drag ratio C_L/C_D .

W cos γ : is the weight component on the vertical axis, for cruise condition or when the aircraft is rolling on the runway, γ is zero, so $W \cos \gamma$ becomes simply W , and the lift force (or ground reaction if the aircraft is on the ground) equals the weight of the aircraft.

$m \left(\frac{dv_y}{dt}\right)$: This term defines the vertical acceleration of the aircraft. Usually the aircraft will climb at a constant rate, so the variation of vertical speed with time is very small or zero.

The general case of Eqs. (1) and (2) can define any of the 6 defined flight phases [20]:

- Start-up and Taxi out
- Take- Off and initial climb to 3,000 ft.¹
- Climb from 3,000 ft. to cruise altitude
- Cruise at selected speed and altitude
- Descend to 3,000 ft.
- Taxi-in.

Based on Eqs. (1) and (2), *Hermes* iteratively calculates the aircraft performance for a given range or fuel capacity, by performing aerodynamic calculations while using appropriate values of thrust for the corresponding

¹ Normally initial climb is taken to an altitude of 1,500 ft. but in this analysis 3,000 ft. is considered as water is injected from 0-3,000 ft.

engines. Further details of this methodology can be found in Refs.[19,22,23]. Igie et al [21] highlights the different modules of *Hermes*, showing their interactions, with details of the calculation procedures.

2.2 Aircraft Selection and Specification

The NBA chosen and modelled was based on the design of the Airbus A320-200 (CEO) and applicable to SHM and MHM, while the WBA applicable to the MHM and LHM was simulated based on the Boeing 787-9. To date, the A320 is the most common aircraft in the world, and hence the selection. The A320 design has undergone improvements over the years but still represents a modified version of an aircraft which was first flown in 1987. On the other hand, the B787 represents more design modifications: 50% of its weight is from composite materials [24]. It also comprises of more flexible and thinner wings at the tip and new engines with higher by-pass and pressure ratios. All of these combined makes the 787 up to 20% more fuel efficient than its predecessor. Double floor airliners like the Airbus A380 or the Boeing 747 were not considered, as they only represent 5% and 1% respectively, of the WBA order backlog, in contrast to the 28% that the Boeing 787 represents [18]. The information to model both aircraft is summarized in Tab. 1 and was obtained from official documents and reports [25–29]. The payload-range diagram for the NBA was obtained and compared to published data for an A320-200 weight variant 15 with no extra central tanks [27].

Table 1 Aircraft specification and limit requirements

	NBA (A320-200)	WBA (787-9)	Source
Fuselage Length (m)	37.57	62.8	[28]
Wing Span (m)	34.09	60.12	[28]
Empty Weight (kg)	42,200	128,850	[27][29]
MTOW (kg)	78,000	254,011	[27][29]
Max Payload (kg)	20,400	52,587	[27][29]
Max Fuel (kg)	18,729	101,456	[27][29]
Ferry Range (km)	6,667	17,223	[27][29]
Max PL Range (km)	3,815	9,722	[27][29]
Max Passengers	180	381	[27][29]
Order Backlog Share	44% narrow-body	28% wide-body	[18]
Engines	CFM-56-5B	Trent 1000-G	[28]
First Flight	1987	2009	[28]

The validation is achieved by means of Fig.2 where the performance of the aircraft under different payloads is evaluated. The numbers represent the relative error between the modelled aircraft and the source. This shows a maximum error of about 3.6% overestimation at 20,400 kg, which is the maximum payload. The main implication of this is on the fuel estimation, however, does not have a significant influence when comparing the wet and dry cases, where deltas and percentage changes are of interest. Similarly, the model for the WBA was developed and compared to a Boeing 787-9. The differences were of similar magnitude as follows: 5.2% at point B, -2.1% at point C and -6.9% at point D.

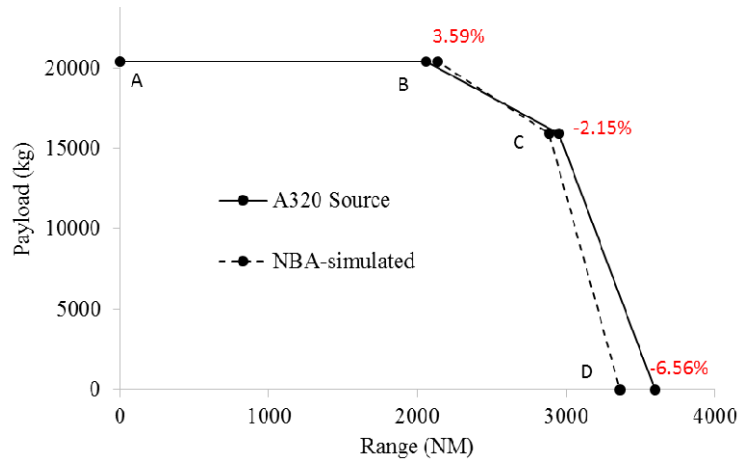


Figure 2 Payload-Range Diagram for NBA

2.3 Added Weight due to the Water Injection system

An estimation of the water injection system weight was subsequently calculated and added to the original aircraft weight. A system design was developed based on the assumptions found in Daggett [17]. The study indicates a detailed analysis of water injection design for a Boeing 747-400ER. The weight of the pipes and tanks in the present study were scaled based on the required water volume and the wingspan of each aircraft. It was initially assumed that the amount of required water was 2% of the core air mass flow at full thrust, applied for 2.9 minutes (0.7 for take-off and 2.2 minutes for the initial climb) according to ICAO EEDDB [31]. This is a conservative assumption as the thrust for take-off and climb will be below the maximum take-off thrust. As such, the air mass flows are actually lower. In absolute terms, the amount of water will be also lower when using the water-to-air ratio relationship. According to Ref. [31], the climb segment occurs at 85% of the maximum thrust. For the case of the NBA, the initial calculation showed that 500 kg of water were needed to cool the engine during take-off and early climb. However, when the simulations performed on *Hermes* for the aircraft operation, it was shown that this value is, in fact, closer to 300 kg. The lower value is a consequence of the thrust of the engine being below 100% for the segments going from 0-3,000 ft. Regardless of this, the water weight on the simulations was kept constant and assumed to be 500 kg to keep the estimations conservative (allowing for an additional 200 kg of equipment). The weights of the pumps were calculated by analysing the specifications of fuel pumps for different aircraft [32]. The final weight breakdown is given in Tab. 2, where the original system for the B747 is compared.

Table 2 Water Injection system weight

	Original System 747 [17]	System for NBA	System for WBA
No. of engines	4	2	2
Pump (per engine) (kg)	12.47	10	14
Tanks and mounts (kg)	79.38	26.27	42.69
Valves, wires, tubes(kg)	151.95	69.74	93.49
Hydraulic accessories*(kg)	25.40	25.40	25.40

System weight - empty (kg)	306.63	141.41	189.58
Water, Max (kg)	1514.16	501.12	814.32
Total Extra Weight (kg)	1820.79	642.53	1003.9

* Includes, distribution valves, manifold, water mixers, flow meters, pressure gauges etc.

The weight of the empty tank system is added to both aircraft in the form of extra payload for simulation purposes. It is assumed that at the beginning of the take-off roll, the system is full of water and thus the weight increase will be 642 kg and 1,003 kg respectively for the NBA and WBA. The water will be consumed during take-off and climb, up to 3,000 ft. As the gradual/momentary reduction in weight due to the water being consumed cannot be simulated in *Hermes*, it is assumed that from 0-3,000 ft., the aircraft carries the full weight of the system (plus the water). From 3,000 ft. onwards, only the weight of the empty system is accounted for. Simulations were done for the take-off roll, with and without the water weight, but considering the system weight. This was done to evaluate the error in assuming that the water is suddenly consumed at 3,000 ft., rather than being gradually used. These did not cause a considerable error when calculating fuel consumption difference between the two cases (0.9% for that segment). The total increase in weight is only 0.99% for the NBA considering the longest mission studied. For the WBA, it is 0.46% for the longest mission.

2.4 Performance of Aircraft with Compressor Water Injection

The performance of the aircraft for water injection was calculated by coupling three platforms: the stand-alone compressor evaporative model [33], the stand-alone engine performance model [34] and the aircraft model introduced in this paper. The simulation procedure for the aircraft with water injection is as follows:

- 1- A baseline mission with the unmodified aircraft is calculated and used as a reference as shown in Fig. 3 from left to right of the figure.
- 2- Another identical mission is calculated for the aircraft with the extra system weight.
- 3- The thrust values required, along with the environmental conditions and compressors pressure ratios and efficiencies of step 2 are recorded and used as boundary conditions for subsequent steps (stand-alone engine). This is conducted only for the take-off roll and climb up to 3,000 ft.
- 4- The performance of the stand-alone compressor (with evaporation model - under the same operating conditions as step 3) is calculated assuming water injection at a rate of 2% of the compressors air mass flow with 5 μ m droplet size. The compressor discharge temperature (CDT) change is computed using the methodology found in [33]. This is the boundary condition required for the engine model for water injection in the next step.
- 5- The outcome of step 4 is imposed on the engine model to account for water injection and the performance of the water injected engine is computed using *Turbomatch*, following the methodology found in [34]. This is also achieved keeping the thrust consistent with step 2 and 3.
- 6- The difference in performance between the “dry” and the “water injected” engine is recorded and applied to step 2.

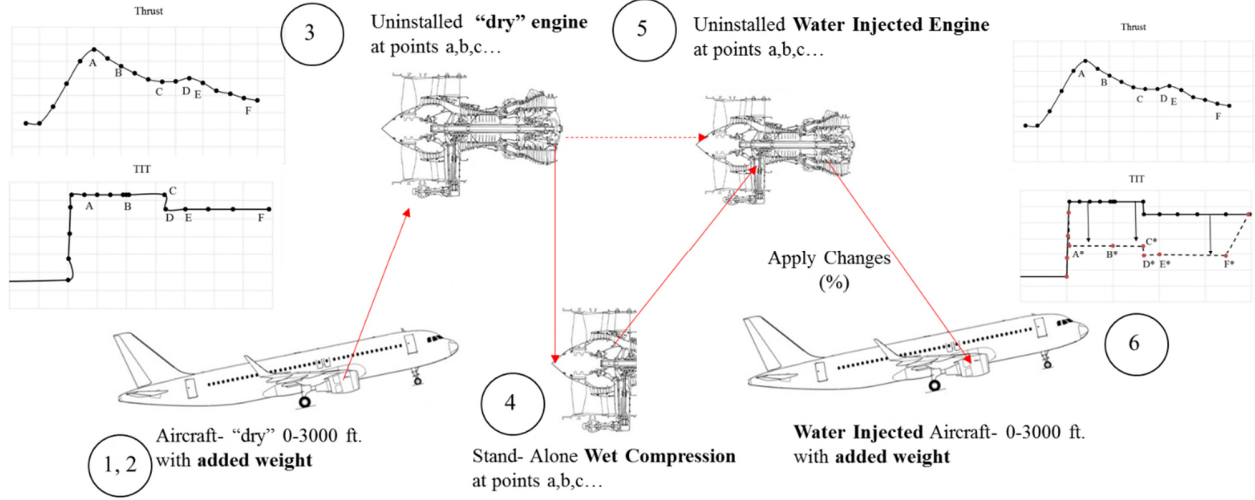


Figure 3 Simulation procedure for the aircraft with water injection

Further information about the compressor and the engine models can be found in Refs. [33,34], that consist of the same conditions of water injection investigated here. Details of the engine design and off-design points and their comparison against available data for similar engines can be found in Appendix A.

2.5 Emission Modelling- Landing and Take-Off Cycle.

The primary aim of water injection at the start of the investigation from the previous works [33,34] has been to reduce NO_x emissions. The associated fuel savings are obtained only during take-off and early climb. In this section, the attention is on the Landing and Take-Off (LTO) Cycle that focuses on the emissions around the proximity of an airport. Correlations of emission indices of NO_x to combustor inlet temperature were created based on the experimental results published by ICAO [31] and following the methodology found in Refs. [35,36]. For the 2-spool engine installed on the NBA and based on the CFM56-5B engine:

$$EINO_{xcalc} = 0.000175 * Tb^2 - 0.14809 * Tb + 35.09184 \quad (4)$$

That of the 3-spool engine installed on the WBA, based on Trent 1000-G engine is:

$$EINO_{xcalc} = 0.00039 * Tb^2 - 0.43532 * Tb + 126.99 \quad (5)$$

Where, T_b is the combustor inlet temperature, which was obtained from simulating the engine performance at 7%, 30%, 85% and 100% of the maximum take-off thrust, corresponding to the four power settings defined in the ICAO EEEDB [31]. The correlations were then validated for both engines against the published data of Ref. [31] as shown in Fig.4.

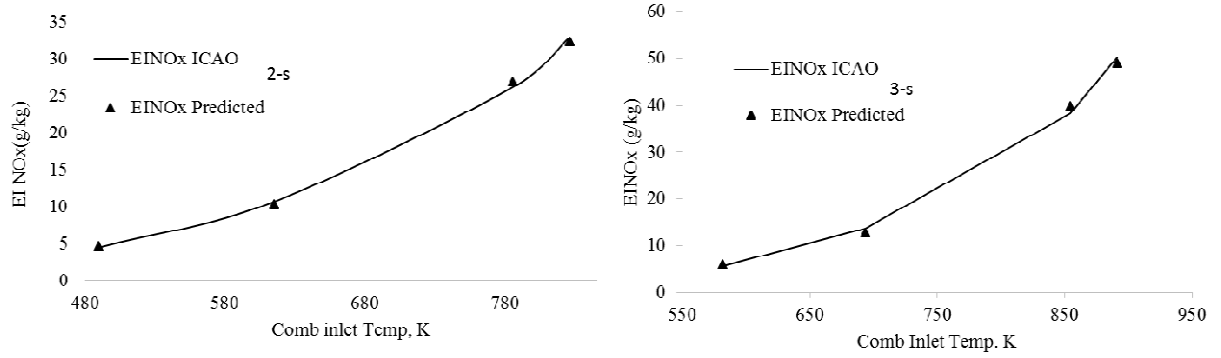


Figure 4 Prediction of NO_x for the 2-spool (left) and 3-Spool engine (right)

Unlike a stand-alone engine study as in Ref [34] for the aircraft-engine configuration, the Mach number, altitude and thrust levels of the engine will change with time. Equations 4 and 5, can account for the engine operating point changes by adjusting T_b , however, they need correction for the change in humidity and pressure with altitude as shown in Eq. 6 [36].

$$EINOx_{corrected} = EINOx_{calc} * \left(\frac{P_{ref}}{P}\right)^{-0.5} * e^{-(19*(w-w_{ref}))} \quad (6)$$

Here w is the humidity content of the air, defined as the mass of water vapour (in kg) per kilogram of dry air. P_{ref} and w_{ref} are the combustor inlet pressure and ambient specific humidity for the engine running at maximum thrust on ISA sea level conditions of 288 K and 60% RH.

For the case considered, w is the sum of the atmospheric water vapour, plus the injected water. The injected water is constant and for the cases studied, has been defined as 0.02 kg of water per kg of air (2%). The atmospheric absolute humidity is defined by the ambient temperature and relative humidity and it decreases with altitude [35]. A relationship was derived based on the information found in Ref [35] to consider the variation of humidity with altitude up to 3,000 ft. More details of the calculations of the atmospheric humidity can be found in Appendix B.

The total NO_x can be calculated by multiplying the Emission Index (grams of NO_x per kg of fuel) by the fuel used in that segment, mf as indicated in Eq.7. The summation of the different segments, i , will give the total NO_x emissions per flight phase.

$$mNOx(g) = \sum_{i=1}^n (Mf_i) * (EINOx_i) \quad (7)$$

2.6 Missions and Engines Investigated

Five missions have been considered as shown in Tab 3. Short and Medium-Haul missions (SHM, MHM) are applicable to the NBA, and Medium and Long-Haul missions (MHM, LHM) are applicable to the WBA. The range classification is based on Eurocontrol; short-haul: airport to airport distance is less than 1,500 km; medium-haul: distance more than 1,500 km but less than 4,000 km; and long-haul, distance is more than 4,000

km [37]. The justification for these missions is to investigate the influence of water injection on mission duration or range. This is of interest as water injection is shown to improve fuel efficiency [14,16,34] but the overall implications of carrying the empty injection system and its implication on mission performance are of interest here. It is also of interest to see if the fuel savings identified in the previous studies [34] offset the expected weight penalty that will be worsened by increased distance. Table 3 indicates the engine models used. These engines are also applicable to the respective aircraft type in actual practice. The referred studies [33,34] shows the impact of water injection on the stand-alone engine and the case applied in this study is that of ISA conditions (288 K, 60% RH).

Table 3 Missions Investigated

Case	Mission	Distance (km)	Aircraft	Engine Model*
1	SHM (e.g. London to Paris)	522	NBA	2-Spool [34]
2	SHM (e.g. London to Barcelona)	1,249	NBA	2- Spool [34]
3	MHM (e.g. London to Beirut)	4,054	NBA	2- Spool [34]
4	MHM (e.g. London to Beirut)	4,054	WBA	3-Spool [34]
5	LHM (e.g. London to Tokyo)	11,349	WBA	3-Spool [34]

4- Results

4.1 Impact of WI on Take-off Performance

The impact of water injection on take-off performance is investigated in this section. Fig 5 shows the net thrust, TIT and the corresponding altitude throughout a complete flight mission. This mission relates to Case 3 of Table 3. This is the baseline aircraft with no water injection with a full payload of 20,400 kg. The highest level of net thrust (134.2 kN) is seen to occur at the beginning of the take-off roll when the aircraft experiences the highest acceleration. As the altitude increases, the net thrust decreases due to the decreasing air density (along with aerodynamic drag). The climb segment is regulated to a fixed calibrated airspeed (CAS) and climb rate, to keep the noise levels down as in practice. As shown for the climb, the TIT is kept constant, allowing for this decreasing thrust with altitude. The maximum values for the engine operating temperature are restricted in both, the temperature itself, and the duration. When the aircraft reaches the cruising altitude of 10,886 m (35,700 ft.), the net thrust levels are seen to be considerably reduced as the thrust required at this stage is only that needed to overcome the drag, at this segment of the flight the aircraft is not accelerating nor climbing. At descent, the thrust levels are generally lower than any segment of the mission, as the gravity term in Eq. 1 and 2 is now in the direction of travel, and adds to the thrust term. As the aircraft descends in altitude, the air density and thus mass flow into the engine will rise. The latter effect should cause an increase in net thrust that is not observed here due to the reduction in the power setting of the engine by means of fuel flow reductions (and thus TIT). After touchdown, the thrust reverser is deployed to decelerate the aircraft, this is represented by the peak seen just after the 300th minute of the mission.

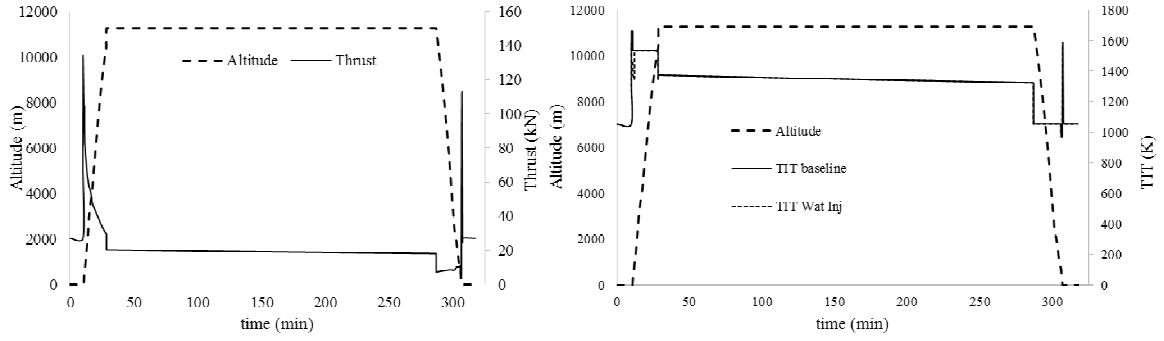


Figure 5 Left: Altitude and Net Thrust vs time. Right: TIT and altitude vs time for complete mission – Case 3

For water injection (applicable to all cases simulated in this study) the baseline net thrust is maintained and so the effects of injecting water will be reflected in a lower engine operating temperature and lower fuel consumption. The calculations involving the water injection case are obtained from the individual point calculations, arising from the specific altitude, ambient condition and the power setting of the baseline case. These individual point calculations are signified on Fig.6 by markers, and are obtained as explained in the previous section. Using Eq. 8, the additional fuel flow as an effect of the extra weight can be calculated for case 3. If the aircraft had the extra weight (water + system), but the water system was turned off, during the take-off segment (up to 3,000 ft.) the extra fuel required amounts to 3.5 kg (+1.27%). For the entire mission, this is 24 kg, noting that beyond 3,000 ft., only the system weight without water is the penalty. Hence, the effect of the added weight though small as indicated has been accounted for. Since the “water injected” aircraft is slightly heavier than the baseline, the take-off and climbing duration is expected to be longer, though observed to be insignificant (this is 2 and 3 seconds for the NBA and WBA, respectively). This marginal increase in time will have a small impact on the fuel utilised, also accounted for. The segment fuel is calculated by means of Eq. 8, which represents the summation of the fuel flow at each segment multiplied by the segment duration. Where M_f is the total fuel weight, FF is the fuel flow and can be obtained by multiplying the SFC by the thrust of each engine, t is the segment time and n is the number of engines.

$$M_f = \sum_{i=1}^n \frac{1}{2} (FF_i + FF_{i+1}) * (t_{i+1} - t_i) * n \quad (8)$$

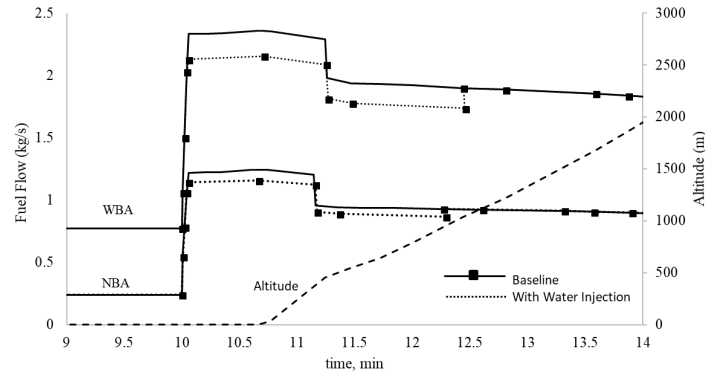


Figure 6 Fuel flow vs time for take-off and initial climb - Case 3 and 4 (NBA and WBA)

Figure 6 indicates the fuel flow during the take-off and early climb segment for Case 3 and 4 applicable to both aircraft. As shown in the figure, when the engine runs at full thrust, the water injection system is turned on, resulting in reduced fuel flow for the segments going from 0 to 1,000 m or just above 3,000 ft. This reduced fuel flow reflects an increase in the thermal efficiency of the power plant for a constant thrust. This has been influenced by a reduction of the specific compressor work by means of the intercooling effect of the evaporating water that increases the air mass flow. Once the aircraft climbs above the regulated emission altitude of 3,000 ft. (after 12 mins, including taxiing) the system is turned off, also assuming all the water is consumed. Figure 6 also indicates that a reduction in fuel flow is higher for the WBA than for the NBA. This higher reduction is due to the different engine architecture found on each aircraft. Block and Igie [34] explains the justification of this, indicating that the advantage of WBA engine of three-spool design over the two-spool in the NBA engine, is the higher operating temperature and pressure, overall leading to faster evaporation. As a result of this effect, in absolute terms for the take-off roll, water injection would result in 14.8 kg less of fuel used for the NBA (Case 3) compared to 48 kg for the WBA. The difference in engine compressor architecture and pressure ratio leads to different temperature reductions when injecting the same water-to-air ratio. This is reflected in the specific compressor work reduction which directly impacts the fuel flow, and is also reflected in the Compressor Discharge Temperature (CDT) as shown subsequently.

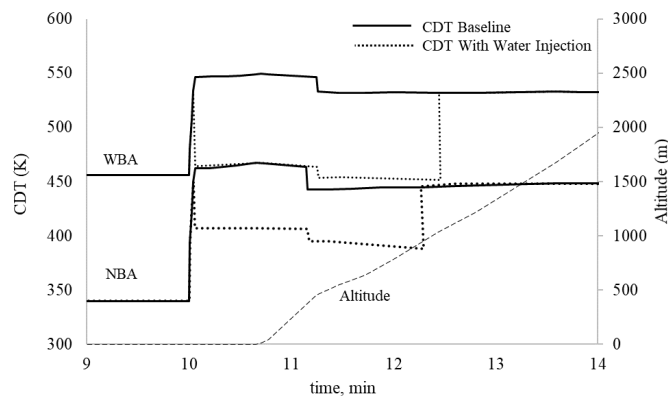


Figure 7 Intermediate CDT for take-off and initial climb - Case 3 and 4 (NBA and WBA)

Figure 7 shows the resulting intermediate CDT due to water injection compared to the baseline case for both aircraft. A drop of 60 K and 82 K is seen for the NBA and WBA respectively. The lower temperature gas delivered into subsequent components of the engine will result in an overall reduced temperature operation. As indicated in Fig.8, the WBA engine has a take-off TIT almost 200 K greater than the NBA engine for baseline operation (due to higher pressure ratios). However, similar to the CDT reductions, the TIT reductions are greater for the WBA than for the NBA. This is a 195 K and 250 K drop in TIT for the NBA and WBA aircraft respectively. These reductions are consistent with Daggett et al. [38] and Sun et al. [14] for engine point calculations. From the figure, it can also be inferred that injecting water into the compressor allows for a larger margin between the operating temperature and the maximum allowable TIT. These improvements suggest that that aircraft will be able to take-off in hot conditions without the need of reducing the payload.

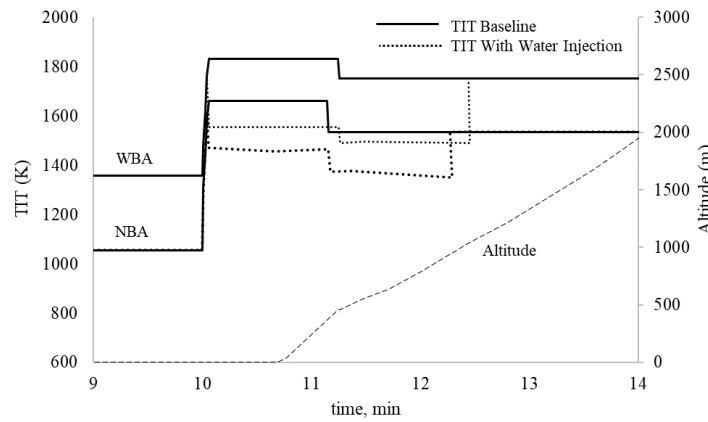


Figure 8 TIT for take-off and initial climb - Case 3 and 4 (NBA and WBA)

4.2 Influence of mission range

The take-off segment fuel savings seen in Fig. 6 are counteracted by a fuel penalty derived from carrying the extra weight of the empty water injecting system throughout the rest of the mission. The longer the range of the mission, it is expected that the penalty will increase. The balance between the fuel savings (during take-off and climb) and the fuel penalty is of interest, and all cases indicated in Tab. 3 are presented here. The fuel changes for each segment of the flight are shown in Fig.9, as well as the total or overall effect, compared to a baseline case that flies the same mission but does not have water injection. The columns in the figure for each case (1-5) represent the fuel changes at each flight segment: 0- 3,000 ft.; 3,000 ft. to cruise; cruise, descend, and finally the combined effect. Similar to previous simulations, the payload is unchanged and the water injecting system is an extra weight to the aircraft's baseline take-off weight. This weight is estimated from the sum of the reported aircraft and engine weight [27,29], the maximum payload weight, the water injection system and the fuel weight. The latter is iteratively calculated by *Hermes* so that only the fuel required for the mission, plus the contingency fuel is considered. From 0 to 3,000 ft., there is a considerable fuel saving in all the cases despite the extra water weight. This reduction in segment fuel is a consequence of the reduced compressor work discussed in earlier sections. The reduction generally increases with mission range as seen; though, for the WBA, its MHM shows a marginally higher reduction than the LHM. Case 3 shows a higher fuel reduction (during take-off) than case 2, and case 2 larger than case 1. This increasing trend has to do with the aircraft

taking off heavier, due to more fuel required to complete a longer mission. Since the maximum thrust that the engines can output is the same in all the cases, a heavier aircraft will take longer to take-off and climb. For this reason, water will be injected for a longer period of time, hence the apparent higher fuel reductions seen in case 3 (-5.07%) compared to case 1 (-4.43%).

Beyond 3,000 ft. to maximum climb or start of cruise, it can be seen that there is a fuel penalty. This increases gradually with range from case 1 to case 3 (for the NBA) due to an increase in duration of this segment with an increase in range. Case 2-5 reflects an increase in cruise duration leading to an increase in the penalty of fuel consumption. The overall impact is depicted in the last column of each case, and observed to be most favourable for the shortest duration – case 1 with 0.42% reduction in fuel, and the worse for case 3, which is slightly penalized with 0.04% increase in fuel. When comparing the same range as case 3 and 4 applicable to the 2 and 3-spool or NBA or WBA respectively, the latter outperforms. This is attributed to the better efficiency of the engine as discussed in Ref [34]. Cases 4 and 5 applicable to the WBA also highlights the favourability of shorter range with regards to the impacts of water injection. The penalty during the cruise for the WBA (Cases 4 & 5) is seen to be small, since this is a heavier aircraft and the proportion of the water injection system weight, compared to the aircraft weight is much smaller (0.1% of the Take-Off Weight) than what was seen for the NBA.

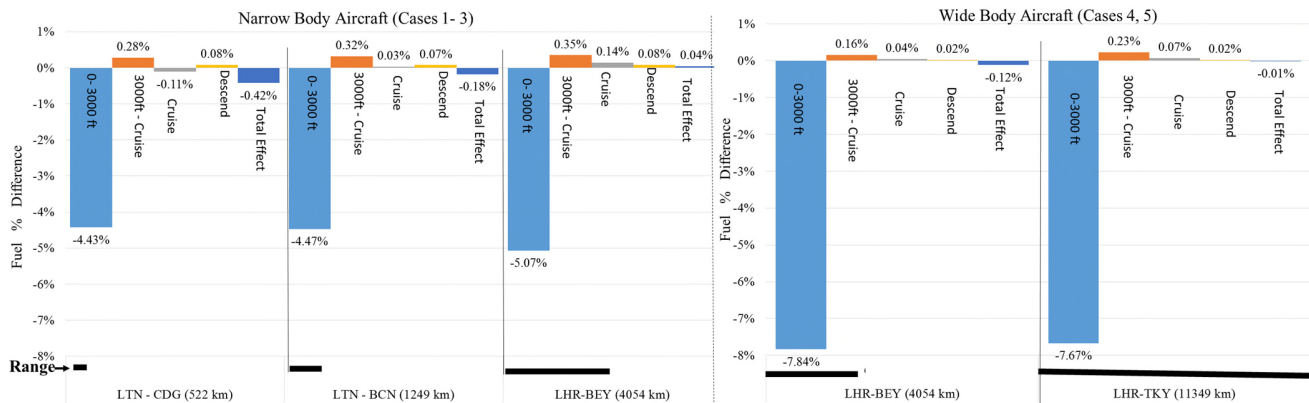


Figure 9 Impact of water injection additional weight on the range fuel flow per flight segment and overall mission

Table 4 shows the baseline and water injection total mission fuel burn for each case. The Carbon Dioxide (CO₂) emissions are also displayed by assuming that 1 kg of kerosene generates 3.16 kg of CO₂ [39].

Table 4 Total Fuel Burn and Carbon Dioxide emissions per mission

	Case 1 522 km	Case 2 1,249 km	Case 3 4,054 km	Case 4 4,054 km	Case 5 11,349 km
Fuel (kg) Baseline	2,898	4,766	12,765	28,430	77,915
Fuel (kg) Water Injection	2,886	4,757	12,770	28,397	77,907
CO ₂ (kg) Baseline	9,158	15,061	40,337	89,839	246,211
CO ₂ (kg) Water Injection	9,120	15,032	40,353	89,735	246,186

Further context to be noted with regards to the assumption of a constant payload in this study that does not involve the reduction of passengers to accommodate for the added weight of the injection system is as follows:

- An Airbus A320-200 (NBA here) is certified to evacuate 180 passengers [25] and the cabin of the A320 fleet used by the low-cost carrier EasyJet is configured to maximize the passenger utilization. The load factor of this specific airline for the years ending 2016 and 2017 is of 91.55% on average [40]. Based on a yearly average, the aircraft are 15 passengers short of their full capacity. In addition, a NBA like the A320 or the B737 is normally used for short-haul trips, for which the take-off fuel is below the maximum fuel weight allowance. EasyJet's average sector distance in 2017 was 1,050 km, that is one-quarter of the aircraft maximum-payload range [41]. For these reasons, it is unusual that these NBA will take-off at their MTOW; an observation also made by Koudis et al. [6] where the take-off weights and thrust settings for more than 3 thousand flights are reported. The article shows that these types of aircraft usually take-off around 85-95% of their weight capacity. If there were ever 100% of MTOW, 8 passengers would have to be removed (constituting 4% decrease in capacity) from the aircraft for it to comply with the original take-off weight (assuming that an average passenger with carry-on bag will weigh 83 kg [42] to make up for the 642kg indicated on Tab.2).
- For the WBA, the extra weight at take-off would be 1,004 kg if allowed, which equates to 12 passengers with no check-in baggage (that is unlikely on a long-haul flight). A 787 on a MHM and LHM considered here is certified to evacuate 381 passengers [26]. Hence a reduced number of passengers would represent 3% of its maximum capacity. However, the passenger load factor for a long-haul airline carrier like British Airways is 81.2% (2016) [43]. This translates to 72 passengers for an aircraft like a 787-9. Despite the fact that the fuel capacity might be at its maximum weight for long-haul flights, the 2, 3 or 4 class cabin configuration means the aircraft is unlikely to carry the maximum number of passengers that it is certified for. The 787-9 used by British Airways (4 class configuration) can carry a maximum of 216 passengers which is 165 less than the maximum aircraft capacity.

From these considerations, it appears less likely that a situation would present itself in which passengers would have to be let off the flight to accommodate for the water injection system to avoid exceeding the MTOW. However, if this situation arises, the estimates indicate that the aircraft would have total mission fuel savings between 0.5 and 1%, depending on the aircraft type and the range. These values are obtained by reducing the aircraft payload in an amount equal to the weight of the water plus the equipment. The values are more optimistic than those seen on Fig.9, since the aircraft would be flying lighter than the baseline presented in this study. For example, if the water and equipment weight is 1,000 kg, and 12 passengers are taken off the flight,

the take-off weight at the beginning of the take-off run would be the MTOW; but after the aircraft passes 3,000 ft., it would be flying 812 kg lighter than its baseline case, since the water would be consumed.

An alternative solution commonly used by airline operators to reduce emissions and engine operating temperature (and thus maintenance costs) is reduced-thrust take-off. To achieve this, the pilot enters on the aircraft flight computer an ambient temperature above the actual Operating Ambient Temperature (OAT); the aircraft then restricts the maximum take-off thrust so that the Exhaust Gas Temperature (EGT) margin is respected at this virtual OAT [44]. This reduction in thrust is restricted by the civil aviation authorities to 25% of the maximum thrust [45], and it is limited by the runway conditions (wet, ice or contaminated), the ambient temperature, the wind intensity and direction, the airport altitude and the aircraft weight.

Calculations for take-off derate of 10% and 25% were done for both aircraft (cases 3 & 4) and are presented in Appendix C. Results show that the reductions in temperature obtained from water injection are comparable to those obtained by a 25% reduction in take-off thrust. However, reducing the take-off thrust was seen to increase the take-off and climb times in up to 30%. This time increase has been observed to result in a fuel penalty for certain missions. Koudis et al.[6] Observed that although operators can apply a take-off thrust reduction of up to 25%, most pilots will not exceed 10-15%, and the highest reductions in thrust were only seen when the aircraft weight was about 30% under the MTOW. Water injection could offer similar performance benefits as high take-off derates but without the higher fuel penalties and the restrictions of reduced thrust take-off.

4.3 Impact on Emissions for Different Aircraft

The take-off NO_x reduction seen for cases 3 and 4 are indicated in tables 5 and 6 respectively. The first column represents the NO_x emissions emitted considering the ICAO standard times of 0.7, 2.2, 4, and 26 minutes for take-off, climb-out, approach and taxi, at the corresponding published fuel flows and Emission Indices [31]. The second column is the proportion of NO_x emission that each segment emits, compared to the total LTO emissions. On the next columns, the same parameters are shown but this time for the NO_x calculated on the simulation for the baseline case. The last two columns represent the mass of NO_x obtained from injecting water, and the reductions compared to the baseline case (column 3). These reductions are only seen during 0- 3,000 ft., which is when the system is used. There is also a small increment of 0.2% (Tab.5) compared to the baseline case during approach and landing, attributed to the extra weight of the aircraft.

Table 5 LTO NO_x reductions with water injection for NBA –Case 3

	NO _x (g) (ICAO)	% of Total	NO _x (g) Calc. dry (baseline)	% of Total	NO _x (g) Wat.Inj.	Changes compared to baseline
Taxi	1,544.4	10.9%	1,238.3	11.3%	1,238.3	0.0%
0-3,000 ft.	10,907.7	76.7%	8,337.1	76.1%	3,731.8	-55.2%
Approach and Landing	1,771.9	12.5%	1,386.3	12.6%	1,389.5	+0.2%
Total LTO	14,224.0		10,961.8		6,359.6	-42.0%

The take-off and climb-out NO_x reductions (0- 3,000 ft.) are a lot higher for the WBA (Tab.6). This is attributed, to the higher temperature reductions obtained for this engine type and hence the sensitivity of EINO_x to Tb. The overall reduction in LTO emissions, however, seems to be almost the same for both cases, between 42-43%.

This is attributed to the different weights and configurations of each aircraft which result in different take-off, climb-out, and approach times (taxi times are the same in both cases).

Table 6 LTO NO_x reductions with water injection for WBA – Case 4

	NO _x (g) (ICAO)	% of Total	NO _x (g) Calc. dry (baseline)	% of Total	NO _x (g) Wat.Inj.	Changes compared to baseline
Taxi	4,182.9	10.9%	12,423.2	26.6%	12,423.2	0.0%
0-3,000 ft.	29,983.6	78.1%	28,494.4	61.0%	8,358.7	-70.7%
Approach and Landing	4,236.7	11.0%	5,819.2	12.5%	5,824.3	+0.1%
Total LTO	38,403.2		46,736.8		26,606.2	-43.1%

This demonstrates that assuming the ICAO LTO cycle to evaluate this technology in both types of aircraft would be an overestimation. The NBA aircraft, according to the ICAO cycle (Tab.5), will produce 76% of its NO_x from 0- 3,000 ft., 12.5% on approach and 10.9% on taxiing. This proportion matches well with the simulations. In the dry simulated case, 76.1% of the total NO_x emissions occur during take-off, 12.6% during approach, and 11.3% during taxi. The absolute total NO_x values, however, are slightly different because the flight segment times are different; while ICAO assumes prescribed times per segment, for the simulation, these times depend on the environmental conditions, weight and geometry of the aircraft. For the simulated WBA case (Tab.6), the segment corresponding to 0- 3,000 ft. produces only 61% of the NO_x, while taxi accounts for 26.6% and landing to 12.5%. The substantial difference in the distribution of NO_x emissions with segment means that a higher reduction in take-off NO_x, on this aircraft is required to match the overall LTO NO_x emissions reductions seen in the NBA.

Figure 10 is an integration of the NO_x emission indices to the mission profile for the segments going from the take-off roll to 3,000 ft. The figure shows the NO_x Emission Indices for the two aircraft with and without water injection (NBA- Left and WBA- Right). The water injection quantity has been added on the secondary axis to show when the water is turned on and off. The high reductions seen for the WBA become evident in this figure. According to the ICAO emissions certification sheets, the maximum EINO_x for the take-off of the engine installed on the WBA aircraft is 50.3, and 33 on the NBA. The maximum values reported on the figure are similar, corroborating the validation done in Fig.4. When the WBA aircraft operates with water injection, the NO_x Emission Indices are even lower than the dry-case of the NBA aircraft, despite the fact that the engines on the WBA are rated to almost 3 times the thrust and 1.6 times the pressure ratio.

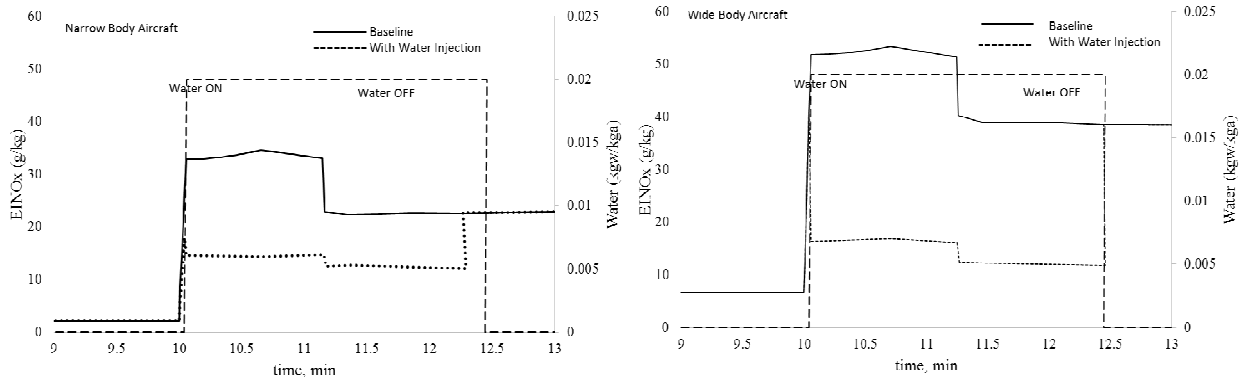


Figure 10 EINOx with and without water injection for NBA (Left) and WBA (Right)

5- Conclusions

The implications of water injection on aircraft performance have been analysed on this study. The case presented here is to maintain the aircraft payload and avoid any thrust augmentation, thereby dropping the specific fuel consumption during water injection. The outcomes of the work have shown that for 2% injection ratio and 5 μ m droplet size:

- The penalty of the additional weight of the injection system leading to an increase in fuel burn can be overcome for the shortest range missions up to 1,249 km. These are ranges in which the take-off and climb segments last for a significant amount of time, in relation to the entire mission duration; as such, shorter cruise. However, this can be extended up to a range of 4,054 km using a WBA powered by a three-spool engine.
- All periods of water injection for any range see a benefit in fuel reduction for their take-off and climb segment up to 3,000 ft. In these instances, the fuel reduction due to water injection outweighs the additional water weight. From 3,000 ft. to maximum climb the opposite is true for all cases of range that water injection is not applied.
- Landing and Take-off (LTO) emissions for NBA or WBA reduces around 42 to 43% for the same MHM.
- Water injection provides similar NO_x and core temperature reductions as a 25% derated take-off, however, it will reduce fuel burn without penalizing the take-off and climb times, and does not have the operational restrictions that reduced-thrust take-off has.
- A positive effect of water injection is the considerable reduction in core temperature. For the NBA, it is a drop in the intermediate CDT and TIT of 60 K and 195 K respectively. For the WBA, it is 82 K and 250 K respectively. These temperature reductions can have significant maintenance costs savings for airline operators as a result of the potential extended creep life of hot the section components.

The take-off time and distance will be influenced by the additional weight of the system. The extra runway length needed for this was evaluated to be no more than 20 m for the NBA and 30 m for the WBA (0.5%-0.75%, considering runway 09L/27R at Heathrow which has a length of 3.9 km).

The droplet diameters considered in this study are 5 μm . In practice, a spraying plume consists of a distribution of droplets of different sizes. As such, the predictions done here are expected to be more optimistic. Doubling the droplet size to 10 μm , assuming no distribution in droplet size, decreases the effectiveness of water injection. Previous work shows a reduction in NO_x decrease from 54 to 50%.

In practice, a Sauter Mean Diameter droplet of 5 μm would be challenging to achieve with conventional injection systems, due to the high water pressure requirements and specialized nozzle design.

Acknowledgements

This work was supported by the Mexican National Council for Science and Technology (Conacyt) and by the Centre for Propulsion of Cranfield University.

Nomenclature

CDT	Compressor Discharge Temperature	MTOW	Maximum Take Off Weight
CEO	Current Engine Option	n	Number of engines
D	Drag Force	NBA	Narrow Body Aircraft
EEEDB	Engine Exhaust Emission Data Bank	NO_x	Nitrogen Oxides
EI	Emission Index	P	Pressure
FR	Friction Force	SET	Small Emitters Tool
g	climb gradient	SHM	Short-Haul Mission
h	altitude	t	time
HPC	High-Pressure Compressor	T_b	Combustor Inlet Temperature
ICAO	International Civil Aviation Organization	TIM	Time In Mode
IPC	Intermediate Pressure Compressor	TIT	Turbine Inlet Temperature
L	Lift Force	TO	Take Off
LHM	Long-Haul Mission	V_x	Axial Velocity
MHM	Medium-Haul Mission	W	Weight
m	mass	w	specific humidity
M_f	Fuel Mass	WBA	Wide Body Aircraft

References

1. ICAO. ICAO Environmental Report 2016- Aviation and Climate Change. 2016.
2. Block N. DA., Igie U. Case For Exploring Compressor Water Injection For Airport Emission Reduction GT2017-64780. In: ASME (ed.) ASME turbo expo: Power for land, sea and air. Charlotte: American Society of Mechanical Engineers (ASME); 2017. p. TBC.
3. Liu Y., Sun X., Vishal S., Nalianda D., Li Y-G., Wang L. Review of Modern Low Emissions Combustion Technologies for Aero Gas Turbine Engines. Progress in Aerospace Sciences. 2017; 94(2017): 12–15.
4. Wulff A., Hourmouziadis J. Technology Review of Aeroengine Pollutant Emissions. Journal of

Aerospace Science and Technology. 1997; (8): 557–572.

5. Koudis GS., Hu SJ., North RJ., Majumdar A., Stettler MEJ. The impact of aircraft takeoff thrust setting on NO_x emissions. *Journal of Air Transport Management*. 2017; 65(X): 191–197.
6. Koudis GS., Hu SJ., Majumdar A., Jones R., Stettler MEJ. Airport emissions reductions from reduced thrust takeoff operations. *Transportation Research Part D*. The Authors; 2017; 52: 15–28. Available at: DOI:10.1016/j.trd.2017.02.004
7. King D., Waitz I. Assessment of the effects of operational procedures and derated thrust on American Airlines B777 emissions from London 's Heathrow and Gatwick airports. Massachusetts; 2005.
8. Ashok A., Balakrishnan H., Barrett SRH. Reducing the air quality and CO₂ climate impacts of taxi and takeoff operations at airports. *Transportation Research Part D*. 2017; 54: 287–303.
9. Zheng Q., Sun Y., Li S., Wang Y. Thermodynamic Analyses of Wet Compression Process in the Compressor of Gas Turbine. *Journal of Turbomachinery*. 2003; 125(3): 489. Available at: DOI:10.1115/1.1575254
10. Bagnoli M., Bianchi M., Melino F., Spina PR. Development and Validation of a Computational Code for Wet Compression Simulation of Gas Turbines. *Journal of Engineering for Gas Turbines and Power*. 2008; 130(1): 012004. Available at: DOI:10.1115/1.2771563
11. Meacock a. J., White a. J. The Effect of Water Injection on Multispool Gas Turbine Behavior. *Journal of Engineering for Gas Turbines and Power*. 2006; 128(1): 97. Available at: DOI:10.1115/1.2032432
12. Utamura M., Takehara I., Horii N., Kuwahara T. A New Gas Turbine Cycle for Economical Power Boosting. *The American Society of Mechanical Engineers*. 1997; 97-AA-142: 1–10.
13. Sexton MR., Urbach HB., Knauss DT. Evaporative compressor cooling for NO_x Supression and Enhanced Engine Performance for Naval Gas Turbine Propulsion Plants. *The American Society of Mechanical Engineers*. 1998; 98-GT332: 1–10.
14. Sun L., Zheng Q., Li Y., Luo M., Wang J., Bhargava RK. Numerical Through Flow Simulation of a Gas Turbine Engine With Wet Compression. *ASME Turbo Expo*. 2012. pp. 1–13.
15. Favorskii ON., Alekseev VB., Zalkind VI., Zeigarnik YA., Ivanov PP., Marinichev D V., et al. Experimentally Studying TV3 117 Gas Turbine Unit Characteristics at Superheated Water Injection into a Compressor. 2014; 61(5): 376–384. Available at: DOI:10.1134/S0040601514050024
16. Daggett DL. Water Misting and Injection of Commercial Aircraft Engines to Reduce Airport NO_x. 2004.
17. Daggett D. Water Injection Feasibility for Boeing 747 Aircraft. Nasa Cr-2005-213656. 2005; Available at: <http://gltrs.grc.nasa.gov/reports/2005/CR-2005-213656.pdf>
18. Flight Global. World Airliner Census 2016. 2016.
19. Nalianda DK. Impact of Environmental Taxation Policies on Civil Aviation. A Techno-Economic Environmental Risk Assessment, PhD. Thesis. Cranfield University; 2012.
20. Jenkinson L., Simkin P., Rhodes D. *Civil Jet Aircraft Design*. 2009.
21. Igie U., Goiricelaya M., Nalianda D., Minervino O. Aero engine compressor fouling effects for short- and long-haul missions. *Proceedings of the Institution of Mechanical Engineers, Part G: Journal of Aerospace Engineering*. 2016; 230(7): 1312–1324. Available at: DOI:10.1177/0954410015607897

22. L. J., Simkin P., Rhodes D. Civil Jet Aircraft Design. 2009. Available at: <http://booksite.elsevier.com/9780340741528/appendices/data-b/default.htm> (Accessed: 26 September 2016)
23. Igie U., Goiricelaya M., Nalianda D., Minervino O. Aero engine compressor fouling effects for short- and long-haul missions. Proceedings of the Institution of Mechanical Engineers, Part G: Journal of Aerospace Engineering. 2016; 230(7): 1312–1324. Available at: DOI:10.1177/0954410015607897
24. Boeing. 787 Dreamliner Family. 2017. Available at: <http://www.boeing.com/commercial/787/#/route-map> (Accessed: 6 November 2017)
25. EASA. Airbus A318-19-20-21 Type Certificate Data Sheet. Blagnac; 2017.
26. EASA. Boeing 787-8, 787-9 EASA Type Certificate Data Sheet. 2017.
27. Airbus. Aircraft Characteristics Airport and Maintenance Planning A320. FRANCE;
28. Jackson P. Jane's All The World's Aircraft 2015-2016. IHS; 2016.
29. Boeing Commercial Airplanes. 787 Airplane Characteristics for Airport Planning 787. 2015.
30. Eurocontrol. Small Emitters Tool (SET). 2018. Available at: <https://www.eurocontrol.int/small-emitters-tool> (Accessed: 5 November 2018)
31. ICAO. ICAO Engine Exhaust Emissions Data Bank. 2013; 0: 2013.
32. EATON. Main Gear Fuel Pumps Manual. Devon: EATON Fuel System Division; 2008. p. 20.
33. Block Novelo DA., Igie U. Aero engine compressor cooling by water injection - Part 1: Evaporative Compressor Model. Energy. 2018; 160: 1224–1235. Available at: DOI:10.1016/j.energy.2018.05.171
34. Block Novelo DA., Igie U. Aero engine compressor cooling by water injection - Part 2: Performance and emission reductions. Energy. 2018; 160(x): 1236–1243. Available at: DOI:10.1016/j.energy.2018.05.171
35. Norman P., Lister D., Lecht M., Parlk K., Penanhoat O., Plaisance C., et al. Development of the technical basis for a New Emissions Parameter covering the whole Aircraft operation: NEPAIR. NEPAIR/WP4/WPR/01. 2003.
36. Marchionna NR. Effect of Inlet-Air Humidity on the Formation of Oxides of Nitrogen in a Gas-Turbine Combustor- TMX-68209. Ohio; 1973.
37. EUROCONTROL. EUROCONTROL Glossary for Flight Statistics & Forecasts. 2005.
38. Daggett DL., Ortanderl S., Eames D., Berton JJ., Snyder CA. Revisiting Water Injection for Commercial Aircraft. World Aviation and Exposition. Reno, USA; 2004.
39. Future AS. ICAO Environmental Report 2016. 2016;
40. Easyjet. Easyjet Traffic Statistics. 2017. Available at: <http://corporate.easyjet.com/investors/traffic-statistics/2017/english> (Accessed: 9 August 2017)
41. EasyJet. EasyJet plc Results for the year ending 30 September 2017. 2017.
42. FAA. Advisory Circular- Aircraft Weight and Balance Control. Aviation. 2005. Available at: DOI:10.1177/004728757301200242
43. British Airways Plc. Annual Report and Accounts Year Ended 31 December 2016. London; 2016.

Available at: file:///C:/Users/s241630/Downloads/British Airways Report and Accounts year ended 31 December 2016.pdf

44. Ting D. Reduced and Derated Thrust- Operations Course. 2009.
45. FAA. Reduced and derated ,takeoff thrust (power) procedures- AC25-13. 1988.
46. Daly M. Jane's Aero-engines. 2nd edn. IHS (ed.) Janes Information Group; 2015. 449 p.
47. Easa. EASA Type Certificate Data Sheet CFM56-5B and 5C Series engines. 2012.
48. EASA. EASA Type Certificate Data Sheet Rolls Royce Trent 1000 Series Engines. 2013.
49. Mishra R., Beura C. Life Consumption Assessment of a Large Jet Engine. Journal of Failure Analysis and Prevention. 2014; 14: 519–529. Available at: DOI:10.1007/s11668-014-9842-2
50. Hanumanthan H., Stiitt A., Laskaridis P., Singh R. Severity Estimation and Effect of Operational Parameters for Civil Aircraft Jet Engines. Proceedings of the Institution of Mechanical Engineers, Part G: Journal of Aerospace Engineering. 2011; 226(12): 1544–1561. Available at: DOI:10.1177/0954410011424854

Appendix A – Engines used for the Aircraft Models

Table A 1 2-Spool engine simulated vs CFM-56 at DP and OD (NBA aircraft)

Flight Phase, [ref]	Parameter	Value	% Error with Ref.
Cruise (DP) [46]	Thrust (kN)	25.98	4.67%
	SFC	16.98	-0.29%
Take-Off [31,46,47]	Thrust (kN)	133.50	0.19%
	OPR	30.47	-0.45%
	Air Mass Flow (kg/s)	427.70	-1.48%
	Fuel Flow (kg/s)	1.30	1.22%
Top of Climb [46]	Thrust (kN)	28.56	0.91%
	OPR	34.40	-0.48%
Climb to 3,000 ft [31]	Thrust (kN)	113.48	0.13%
	Fuel Flow (kg/s)	1.06	3.12%
Approach [31]	Thrust (kN)	40.05	-0.42%
	Fuel Flow (kg/s)	0.35	3.21%
Idle [31]	Thrust (kN)	9.35	-0.91%
	Fuel Flow (kg/s)	0.11	-6.15%

Table A 2 3-Spool engine simulated vs Trent1000 at DP and OD (WBA aircraft)

Flight Phase [ref]	Parameter	Value	% Error with Ref.
Cruise (DP) [46]	OPR (kN)	50	0.19%
	SFC	14.33	-5.35%
Take – Off [31,48]	Thrust (kN)	323.70	-0.66%
	OPR	42.53	-1.45%
	Air Mass Flow (kg/s)	1211.00	0.09%
	Fuel Flow (kg/s)	2.40	1.79%
Top of Climb [46]	Thrust (kN)	-	-

	OPR	52.00	-0.44%
Climb to 3,000 ft [31]	Thrust (kN)	275.15	-0.95%
	Fuel Flow (kg/s)	1.97	2.35%
Approach [31]	Thrust (kN)	97.11	0.59%
	Fuel Flow (kg/s)	0.65	0.71%
Idle [31]	Thrust (kN)	22.66	1.32%
	Fuel Flow (kg/s)	0.24	-9.24%

Appendix B- Ambient Humidity Correlations

The correlation used to calculate ambient humidity has been compared to that found in the ISO5878 standard as shown in Fig. B1. and also available in Ref.[35]. The range considered for the calculations corresponds to 0-10 km of altitude and the maximum error of any individual point within this range reported in Fig.B1 was 0.4%, at 10km of altitude. This correlation is only valid for the ground level relative humidity of 60% (ISA conditions).

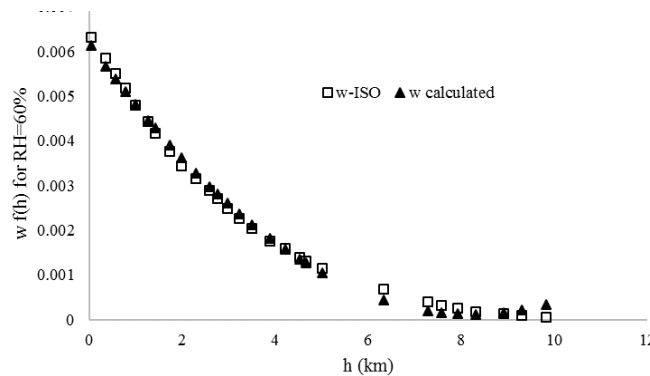


Figure B 1 Variation of absolute humidity with altitude

Appendix C – Reduced Thrust Take-Off vs Water Injected Take-Off

Water Injected (WI) take-off is compared here to reduced thrust take-off (10 & 25%). WI seems to achieve the highest TIT reductions, -196K compared to -165K for the most extreme derate condition. This represents a 12 and 10% reduction, respectively compared to the maximum TIT. Mishra and Beura [49], predicted a 13% reduction in TIT for a 25% derate operation (-228K) with a 2-spool engine installed on a WBA. Hanumanthan et al. [50] report a reduction in Exit Gas Temperature (EGT) of -127K (-11.1%) for a 25% derated take-off on a narrow body aircraft with a 2-spool engine, similar to the one considered here.

Table C 1 Water Injection vs reduced take-off (NBA, case 3)

Average values	10% derate	25 % derate	W. I. (2%)
TIT, ΔT (K)	-69	-165	-196
TIT, %	-4%	-10%	-12%
EGT, ΔT (K)	-31	-70	-104
EGT %	-4.0%	-8.8%	-13.1%

Fuel Flow, (%)	-12%	-28%	-7%
TIM change (%)	11%	36%	1%
TO Fuel change (kg)	-4.58	-5.27	-8.93
TO NO _x change (%)	-20.4%	-43.1%	-58.5%

For the case studied, reducing thrust in 25% would reduce the Take-off (TO) fuel flow by 28%, however it would increase the TO time in mode (TIM) in 36%. This would lead to a total TO fuel saving of -5.27 kg (-4.58 for 10%). Water Injection, despite the extra weight of the water and the system would achieve a TO fuel flow reduction of 7% (4 times less than derated take-off) but no penalty on take-off time, having as a consequence a higher TO fuel saving of -6.9 kg. Some studies, however, report that operations under reduced take-off might incur in fuel penalties associated to the longer take-off and climbing times also seen here [44]. A study made on a fleet of Boeing 777, concluded that a 10% derate could lead to 5.5% increased fuel, and this value can be as high as 15% if full derate (25%) is applied [7]. In terms of NO_x, water injection also seems to deliver higher reductions than reduced take-off. This comes about as a consequence of the high-temperature reduction and the fact that the TIM is not altered with water injection. Table C2, presents a similar case related to a WBA with a 3-spool engine.

Table C 2 Water Injection vs reduced take-off (WBA, case 4)

<i>Average values</i>	10% derate	25 % derate	W. I.
TIT, ΔT (K)	-61.84	-160.61	-274.78
TIT, %	-3.4%	-8.8%	-15.0%
EGT, ΔT (K)	-19.99	-49.99	-130.26
EGT %	-2.5%	-6.3%	-16.5%
Fuel Flow, (%)	-7.09%	-17.79%	0.36%
TIM change (%)	12.2%	41.2%	0.6%
TO Fuel change (kg)	-4.18	1.27	-26.96
TO NO _x change (%)	-19.9%	-43.0%	-69.0%

2019-01-03

On-board compressor water injection for civil aircraft emission reductions: range performance with fuel burn analysis

Block Novelo, David Alejandro

Elsevier

Block Novelo DA, Igie U, Nalianda D. (2019) On-board compressor water injection for civil aircraft emission reductions: range performance with fuel burn analysis. *Transportation Research Part D: Transport and Environment*, Volume 67, February 2019, pp. 449-463
<https://doi.org/10.1016/j.trd.2018.12.021>

Downloaded from Cranfield Library Services E-Repository